Supplement of Solid Earth, 10, 79–94, 2019
https://doi.org/10.5194/se-10-79-2019-supplement

Solid Earth Open Access EGU

Supplement of

Correlation between tectonic stress regimes and methane seepage on the western Svalbard margin

Andreia Plaza-Faverola and Marie Keiding

Correspondence to: Andreia Plaza-Faverola (andreia.a.faverola@uit.no)

Table S1: Tectonic model model parameters for the two rectangular planes (Okada, 1985) used to approximate the deformation due to oblique spreading along Molloy Ridge (MR) and Knipovich Ridge (KR)

Ridge	Length (km)	Depth to lower boundary (km)	Depth upper boundary (km)	Dip (°)	Strike (°)	East midpoint (UTM, m)	North midpoint (UTM, m)	Right-lateral motion* (mm/yr)	Vertical motion (mm/yr)	Opening* (mm/yr)
MR	57	900	10	-90	28	380.000	8820.000	1.8	0	13.9
KR	180	900	10	-90	-3	467.000	8616.000	8.6	0	11.1
* Calculated by assuming a half spreading rate of 7 mm/yr in the direction of N125°E on both the MR and KR.										

Sensitivity tests

To test the robustness of the modelling, in particular with respect to the change from tensile stress on the eastern Vestnesa Ridge (Vestnesa Ridge) to strike-slip stress along the western Vestnesa Ridge, we examine the influence of varying the following model parameters: 1) geometry of the Molloy Ridge (MR) and the Knipovich Ridge (KR); 2) orientation of spreading along the MR and the KR; 3) depth of brittle-ductile transformation (upper boundary of planes); and 4) elastic moduli (Poisson's ratio and shear modulus).

Test of model geometry (i.e. orientation of the Molloy and Knipovich ridges)

The orientation of the MR and the KR axes in the preferred model was estimated from IBCAO bathymetry (i.e., the axes were placed along the depressions of the mid-ocean ridges). To test the effect of the geometrical configuration on the resulting stress field we varied 1) length of the ridges' axes (i.e., translated into a rotation of the Molloy transform fault (MTF)), and 2) azimuth of the ridge axes (i.e., 5 degrees clockwise and counter clockwise rotation of the axes and – as an extreme case - a rotation of KR until it becomes parallel to MR). The spreading direction is kept constant at N125°E in all tests. Shortening and lengthening of the ridge axes have an effect primarily on the stress field at the western KR flank (Fig. S1 b-c). The tensile zone on the eastern Vestnesa Ridge remains. The rotation of the ridges causes a slight shift of the tensile zone northward or southward with respect to the Vestnesa Ridge crest, but this is probably mostly an effect of slight shifts in the termination of the KR. (Fig. S1 d-e). The tensile zone remains even in the extreme case, after rotation of the KR until is parallel to MR. (Fig. S1 f).

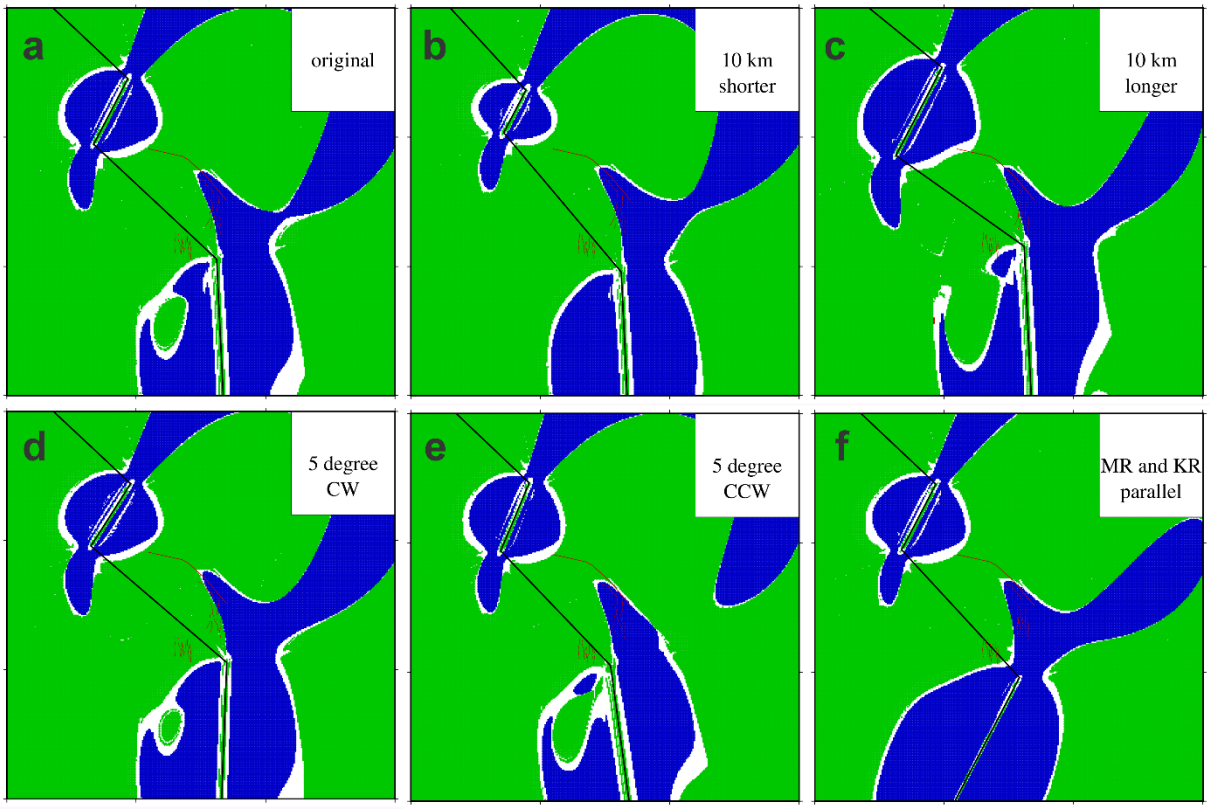

Figure S1: Test of the model geometry: a) preferred model; b) shortening the ridges; c) lengthening the ridges; d) clockwise rotation of the ridges; e) counter-clockwise rotation of the ridges; f) parallel ridges. Green = strike-slip stress, blue = tensile stress, red = compressive stress regime. The crest of the Vestnesa ridge and faults are projected for reference.

Spreading direction of the Eurasian plate with respect to the North-American plate

We used a spreading direction of N125°E along the Molloy Ridge (MR) and the northern part of the Knipovich Ridge (KR) from recent plate motion models by Altamimi et al., (2002), Argus et al., (2010), and DeMets et al., (2010). Other recent plate models give slightly different spreading directions, i.e. N120°E (Drewes, 2009) or N133°E (Kreemer et al., 2014). The direction of N133°E is parallel to the trend of the Molloy Transform Fault (MTF). The use of these alternative spreading directions would either broaden or reduce the zone of tensile stress at eastern Vestnesa Ridge, however, the zone is still present also with a spreading direction of N133°E (Figure S2-c). Changing the spreading rate would only affect the magnitude of the predicted stresses, which are not considered in the present study.

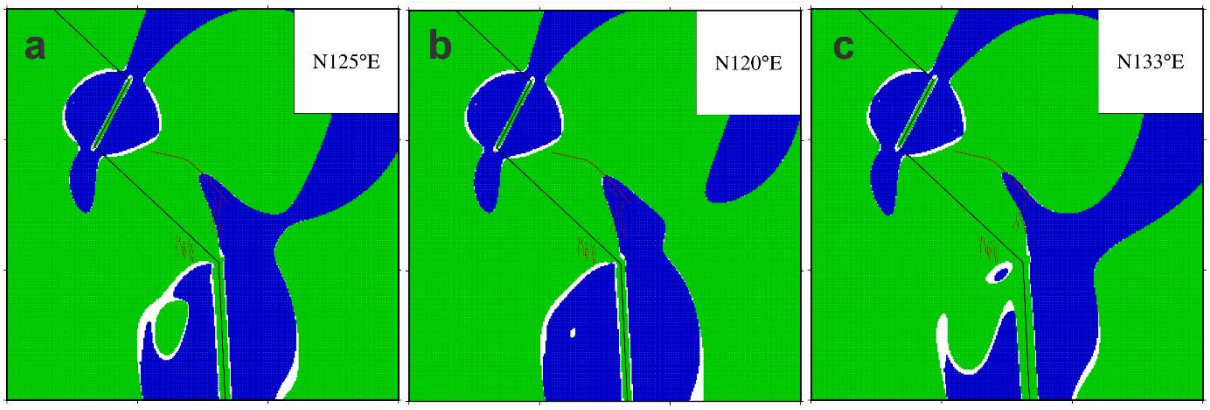

Figure S2: Varying the spreading direction: a) preferred model with N125°E spreading on MR and KR; b) model with N120°E spreading; c) model with N133°E spreading.

Depth to upper boundary (i.e., the depth of the brittle-ductile transition in the model)

The actual depth of the brittle-ductile transition is not well constrained in the study area, but farther south along the Atlantic Ocean, Keiding et al. (2008) estimated the depth along part of the Mid-Atlantic plate boundary in Iceland to be 6-7 km using the same modelling technique and constraint from GPS observations. Hence, the 10 km used in our models may be on the deeper side. Changing the depth to more shallow values, decreases the zone of tensile stress at eastern Vestnesa Ridge, but it is still apparent with an upper boundary depth of 5 km (Fig. S3 c).

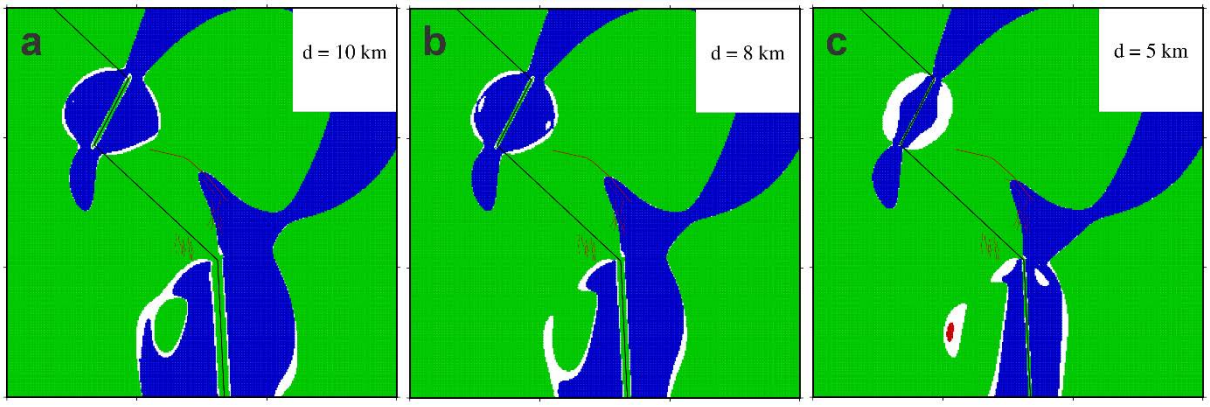

Figure S3: Reducing the depth to upper boundary of dislocation: a) preferred model with 10 km depth to upper boundary; b) model with 8 km depth; c) model with 5 km depth

Elastic moduli

The model takes as input the Poisson's ratio and the shear modulus in the isotropic, homogeneous elastic half-space. The typical range of Poisson's ratio for rocks is 0.1-0.35 (e.g., Gercek, 2007). Varying the Poisson's ration within this range results in markedly different stress patterns to the sides of the spreading ridges, however, the zone of tensile stress at eastern Vestnesa Ridge remains almost unaltered (Fig. S4 b-c). Varying the shear modulus will only affect the magnitude of the predicted stresses, which are not considered in the present study.

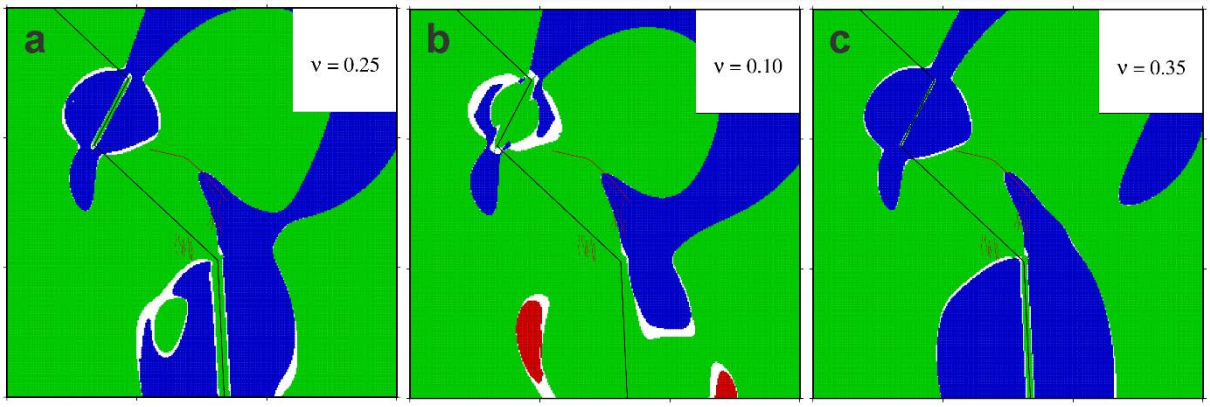

Figure S4: Varying Poisson's ratio: a) preferred model with ν = 0.25; b) model with ν = 0.10; c) model with ν = 0.35.

References:

Altamimi, Z., Sillard, P., and Boucher, C., 2002, ITRF2000: A new release of the International Terrestrial Reference Frame for earth science applications: Journal of Geophysical Research: Solid Earth, v. 107, no. B10, p. ETG 2-1-ETG 2-19.

Argus, D. F., Gordon, R. G., Heflin, M. B., Ma, C., Eanes, R. J., Willis, P., Peltier, W. R., and Owen, S. E., 2010, The angular velocities of the plates and the velocity of Earth's centre from space geodesy: Geophysical Journal International, v. 180, no. 3, p. 913-960.

DeMets, C., Gordon, R. G., and Argus, D. F., 2010, Geologically current plate motions: Geophysical Journal International, v. 181, no. 1, p. 1-80.

Drewes, H., 2009, The Actual Plate Kinematic and Crustal Deformation Model APKIM2005 as Basis for a Non-Rotating ITRF, *in* Drewes, H., ed., Geodetic Reference Frames: IAG Symposium Munich, Germany, 9-14 October 2006: Berlin, Heidelberg, Springer Berlin Heidelberg, p. 95-99.

Gercek, H., 2007, Poisson's ratio values for rocks: International Journal of Rock Mechanics and Mining Sciences, v. 44, no. 1, p. 1-13.

Keiding, M., Árnadóttir, T., Sturkell, E., Geirsson, H., and Lund, B., 2008, Strain accumulation along an oblique plate boundary: the Reykjanes Peninsula, southwest Iceland: Geophysical Journal International, v. 172, no. 2, p. 861-872.

Kreemer, C., Blewitt, G., and Klein, E. C., 2014, A geodetic plate motion and Global Strain Rate Model: Geochemistry, Geophysics, Geosystems, v. 15, no. 10, p. 3849-3889.